IEEE Access
Multidisciplinary ⋮ Rapid Review ⋮ Open Access Journal

Received September 2, 2020, accepted September 12, 2020, date of publication September 18, 2020,
date of current version October 14, 2020.

Digital Object Identifier 10.1109/ACCESS.2020.3024846

Probabilistic Peak Demand Matching by Battery Energy Storage Alongside Dynamic Thermal Ratings and Demand Response for Enhanced Network Reliability

MOHAMED KAMEL METWALY[1,2] AND JIASHEN TEH[3], (Member, IEEE)
[1]Electrical Engineering Department, Faculty of Engineering, Taif University, Taif 21974, Saudi Arabia
[2]Electrical Engineering Department, Faculty of Engineering, Menoufia University, Shibin El-Kom 32511, Egypt
[3]School of Electrical and Electronic Engineering, Universiti Sains Malaysia (USM), Nibong 14300, Malaysia

Corresponding author: Jiashen Teh (jiashenteh@usm.my)

This work was supported by the Deputyship for the Research and Innovation, Ministry of Education, Saudi Arabia, under Project 284.

ABSTRACT Battery energy storage systems (BESS), demand response (DR) and the dynamic thermal rating (DTR) system have increasingly played important roles in power grids worldwide. In addition to storing energy, BESS can supply peak demands, thereby reducing the frequency of load interruptions and deferring new asset investments. However, study on the precise BESS sizing (i.e. energy and power ratings) to supply peak demands to improve the security of supply of transmission networks is still lacking. The combined efficacy of BESS, DR and DTR have also never been studied, because their simultaneous deployment has never been considered. The first contribution of this paper is proposing a probabilistic evaluation method to evaluate various combinations of BESS power ratings and energy capacities and determines their impacts on the reliability of transmission networks, in which peak demands are supported by charges stored in BESSs to address the security of supply problem. The second contribution extends the proposed method to examine the effects of deploying BESS alongside DR and DTR. Our results show that the security of power supply improves along with BESS sizing by as much as 37.2%, and that its reliability becomes more significant as its capability grows, with bigger BESS having more detrimental effects towards EENS as it becomes unavailable than smaller BESS does. DTR and DR reduce the requirements of BESS sizing without adversely affecting network reliability.

INDEX TERMS Battery storage, reliability, dynamic line thermal rating, demand response, power system.

I. INTRODUCTION

Under the backdrop of ageing power system assets, distributed generations and demand for the proliferation of smart grids, battery energy storage systems (BESS) have increasingly played important roles in power grids worldwide [1], [2]. In addition to their energy storage function for facilitating renewable integrations [3]–[5], BESSs can also supply peak demands, thereby reducing the frequency of load interruptions and deferring new asset investments [6]. Despite such application, there is still a lack of studies that systematically quantify the energy capacity and power rating of BESSs, both of which undermine the security of supply in BESS-supported systems, especially in meshed transmission networks.

In [7], peak demands are lowered to reduce the energy supply cost, rather than supported by BESS in a security of supply application. As a result, the storage is inadequately sized, and this approach therefore becomes unsuitable for guaranteeing the security of supply applications despite supporting decisions from a purely economic viewpoint. In [8], the size and location effects of BESS in an active distribution network are investigated. In this study, the total energy and power ratings of storages are fixed, and their deployments are not limited by physical sizes and land availabilities, thereby leading to considerations that are more complex than those observed in real-life situations. Based on fixed ratings, the storage energy and power capacities are optimally

The associate editor coordinating the review of this manuscript and approving it for publication was Zhiyi Li.

distributed across the network. A similar study examined a micro-grid containing BESS and distributed generators [9]. Results show that the well-being of the grid is enhanced by increasing the BESS capacities. However, network operators rarely conduct assessments in their cost/benefit analyses. Although BESSs have also been used to accommodate heat pumps and photovoltaic systems based on various combinations of energy and power ratings, whilst considering storage degradations [10], the use of these systems to support load demand or security of supply has never been investigated. Nevertheless, the sizing of BESS has been thoroughly investigated for wind [11]–[13] and solar [14] integrations, but studies on the application of BESS for guaranteeing security of supply remain lacking. In [15], large storages are used to balance and shift the loads on large networks, but similar to the aforementioned studies, the energy and power ratings of the storage device are fixed, and their values are arbitrarily selected.

In sum, the use of precise BESS sizing (i.e. energy and power ratings) to supply peak demands in the context of security of supply has never been examined in the literature. Examinations of transmission networks are also lacking. Therefore, the first contribution of this paper is to present a probabilistic evaluation method for BESS-integrated transmission networks. This method evaluates various combinations of BESS power ratings and energy capacities and determines their impacts on the reliability of power networks in which peak demands are supported by charges stored in BESSs to address the security of supply problem. Several factors, including load demand, BESS and transmission network reliability and BESS operation criteria (i.e. charging/discharging rates and state-of-charge (SOC)), are all considered in chronologically developed scenarios in sequential Monte Carlo (SMC) simulations. BESSs as network reinforcements have several advantages over conventional methods. For instance, these systems can support bus voltages, gain revenue by participating in ancillary service markets, lacks long-term commitments and involves a short planning process before its deployment. The proposed evaluation method also determines the capacity and time required by BESSs to supply peak demands in order to gauge the availability of these systems for ancillary services.

In addition, the simultaneous deployment of BESS, demand response (DR) and dynamic thermal rating (DTR) systems has never been examined in the literature. The effects of DR and DTR on the role of BESS in supplying peak demands also warrants further examination.

Electricity usage patterns demonstrate a particular behaviour. Generally, the demand peaks during early evenings and during either winter (in cold climate countries) or summer (in warm climate countries) months due to the increased usage of heaters and air conditioners during these periods. Although such peaks are only observed occasionally [16], the design of the entire grid, including the generators and transmission and distribution networks, should accommodate these peak demands. Consequently, most power components have been rarely used up to their full capacities, thereby rendering their high costs and slow returns on investment unjustified.

Instead of conventional planning, utilities can apply various DR techniques that aim to manipulate load demand patterns by incentivising desirable consumer behaviour [17], [18]. The most common DR techniques include peak-shaving (PS) and valley-filling (FV), which shift the load demand above a certain percentage of the peak load to off-peak times. Main goals of DR techniques are to shave peak demands in order to increase the adequacy power supply, reduce the occurrence of blackouts, and lessen the dependencies on costly fast-ramping generators in exchange for a low penalty cost on utilities due to interruptions from the normal load usage of customers. DR and BESS can complement each other given their purpose and their energy storage ability, respectively. Instead of fully depending on shifting load demands as in DR, BESS can be used to supply peak demands (i.e. peak matching), which would subsequently reduce the deployment of DR and the frequency of load interruptions. By contrast, the peak demands partially shifted by DR reduces the capacity requirements of BESS in peak matching.

Apart from BESS and DR, the DTR system, which is a line rating technology that allows utilities to take advantage of the line rating variability based on environmental fluctuations, can be deployed, especially on overhead lines (OHL) [19]. Most of the time, DTR systems increase OHL ratings higher than the conventional method (i.e. static thermal ratings (STR)) and unlock the additional power transfer capacity of networks [20]. Given that this newfound capacity increases the power supplied by generators to load points, the frequency of load interruptions and amount of peak loads that require support are both reduced, thereby reducing the deployments of DR and BESS. In few instances, DTR drops below STR, and operating DTR during these instances can prevent circuit overloads and avoid jeopardising system security, which this is impossible in STR based networks [21], [22].

Although the benefits of DTR [23]–[26] and DR [27] are well known, their effects on the BESS peak matching function have never been studied because their simultaneous deployment with BESS has never been considered. Therefore, as its second contribution, this study extends the proposed method to examine the effects of deploying BESS alongside DR and DTR. This extended method allows us to evaluate the combined efficacy of BESS, DR and DTR in enhancing system reliability (i.e. security of supply) by emphasising peak matching instead of peak shaving whilst considering enhanced OHL ratings. As opposed to using these methods individually, their combined application defers network reinforcements and improves customer servicing better than using any of the methods in isolation.

Fig. 1 illustrates the interaction amongst BESS, DR and DTR based on the 24 h demand from a transmission bus bar in Saudi Arabia, and the ratings for a particular transmission line is as shown, which the DTR is determined based on the hourly average of sampled weather conditions. From

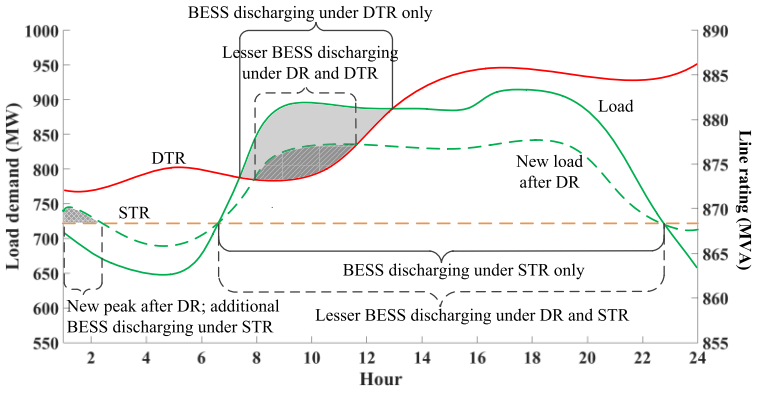

FIGURE 1. Effects of DR and DTR on BESS discharging requirements.

hour 0700 to 1300, the load level surpasses DTR. During this period, DR can perform peak shaving or BESS can be deployed to match the peak demand, with the latter being less obstructive to customers by not imposing a particular demand usage behaviour. The implementation of DR alleviates the energy capacity requirement of BESS as reflected in the reduced area between the load and DTR curves, whilst the maximum power mismatch between load and OHL limit (DTR) is treated as the power rating requirement of BESS. Fig. 1 also shows that when operating with STR, mismatch between rating and load demand (between hour 0700 and 2300) is much larger than if operating with DTR, and the capability requirement of BESS for peak matching is therefore much higher. Although DR can reduce the requirements of BESS in STR, DR may also cause the new load profile to rise above the STR in some instances (between hour 0000 and 0200) due to its low level, thereby offsetting some of the earlier effects of reducing the demand for BESS. This phenomenon can be avoided in the DTR operation and shows that operating with DTR and DR can alleviate both the energy and power requirements of BESS.

II. METHODOLOGY

A. OVERVIEW: ASSESSMENT OF BESS PEAK MATCHING

This paper uses BESS instead of conventional network assets (i.e. more and higher capacity transmission lines) to improve the security of supply of customers. Therefore, the effects of various energy and power ratings of BESS on the power system reliability should be quantified; DR and DTR are considered alongside BESS. A probabilistic method based on SMC is employed to consider the possibilities of large demand variations, the random statuses of power network components and BESS and the chronological developments of events. The reliability of the power network is assessed by adopting the most widely used reliability index, namely, expected energy not supplied (EENS), with a high EENS corresponding to a low reliability, and vice versa. The process of the developed SMC is described as follows:

1) PREPARATION PHASE

1) Prepare hourly demand data for 8760 hours or 1 year based on the allowable peak load specified in the DR model (see *Section II.B* for DR modelling details).
2) Prepare hourly ratings of OHLs for the same timeframe based on the DTR model (see *Section II.C* for DTR system modelling details).
3) Prepare random statuses of OHLs and BESS (see *Section II.D* for BESS modelling details). The reliability of other power components, such as cables, generators and transformers, are not considered to prevent these components from masking the failure effects and capacity limitations of transmission lines (i.e. OHLs) given that this study focuses on assessing the effects of BESS on the security of supply at the transmission network level. However, the capacity limits of these components are still taken into consideration.

Random statuses are generated by using the basic inverse transform method, in which a uniform random number at each hour i, U_i, is drawn between 0 and 1, and the transition time of event, which is either time-to-failure (TTF) or time-to-repair (TTR), is determined as $-ln\,(U_i)\,/x$, where x is the failure rate when generating TTF or the repair rate when generating TTR. The summation of TTF and TTR yields one complete cycle of sequential up-down statuses, and the process of generating both TTF and TTR is repeated until 1 full year is satisfied.

2) EXECUTION PHASE

The effects of all data in the preparation phase are assessed by executing the direct-current optimal power flow (DC-OPF) on the investigated power network. DCOPF is chosen over alternating-current OPF (AC-OPF) for the following reasons: (a) active power is more important than reactive power constraints in long-term reliability studies; (b) DC-OPF is significantly faster than AC-OPF and has previously generated accurate results [28]; (c) generators and reactive power compensators provide adequate support to reactive power demand; and (d) DTR affects only real power limits of OHLs.

As implied by its name, DC-OPF screens for active power violations at every hour of the SMC simulation. In each detected violation, generators are re-dispatched, and then BESSs are deployed to ensure maximum power supply to load demand before load shedding takes place. This OPF protocol minimises load curtailment and is in line with actual power system operations. The function of DC-OPF is expressed as

$$\min\left(\sum_{l\in\Omega_{LB}}|LC_l|\right), \tag{1}$$

which is subject to

$$\sum_{g\in\Omega_G}PG_g+\sum_{j\in\Omega_B}PB_j=\sum_{l\in\Omega_{LB}}\left(PD_l^{DR}-LC_l\right), \tag{1a}$$

$$PG_g^{min}\le PG_g\le PG_g^{max};\ \ g\in\Omega_G, \tag{1b}$$

$$-PR_j\le PB_j\le PR_j;\ \ j\in\Omega_B, \tag{1c}$$

$$SOC_j^{min}\le SOC_j\le SOC_j^{max};\ \ j\in\Omega_B, \tag{1d}$$

$$0\le LC_l\le PD_l^{DR};\ \ l\in\Omega_{LB}, \tag{1e}$$

$$\sum_{i=1}^{n}GSF_{k,i}\times(PG_i-PD_l)\le f_k^{DTR};\ \ k\in\Omega_L, \tag{1f}$$

where in (1), LC is the amount of load curtailment, and Ω_{LB} is the set of all load buses. In (1a), PG_g is the power output of generator g, Ω_G is the set of all generators, PB_j is the power discharged by or charged into BESS j, Ω_B is the set of all BESSs and PD_l^{DR} and LC_l are the power demand profiles modified by DR and the amount of load curtailment, respectively, of load bus l. In (1b), PG_g^{min} and PG_g^{max} are the minimum and maximum capacities of generator g, respectively. In (1c), PR_j is the power rating of BESS j that controls the chargeable/dischargeable power of BESS at any moment. In (1d), SOC_j^{min} and SOC_j^{max} are the minimum allowable and maximum SOC of BESS j, respectively, and Ω_B is the set of all BESS. In (1e), the amount of LC_l is limited by the maximum power demand. In (1f), $GSF_{k,i}$ is the generation shift factor of line k to generator i (limited by the maximum capacity of line f_l^{DTR}, which is based on the values determined by DTR systems), and Ω_L is the set of all transmission lines.

DC-OPF is executed at each hour until the end of the simulation period (i.e. a year), and the amount of power demand and supply mismatched (i.e. energy not supplied (ENS)) during the simulation is recorded. The preparation and execution phases are repeated, and the values of the expected ENS (EENS) are updated each time by considering all previous ENS values. The entire SMC simulation stops when the variation in EENS converges below 5% or after 5000 simulations have lapsed. EENS is formulated as

$$\mathrm{EENS}=\frac{1}{Y}\sum_{y=1}^{Y}\sum_{i=1}^{8760}\mathrm{ENS}_i. \tag{2}$$

Fig. 2 shows the algorithm of the proposed method for assessing the EENS of a power network whose security of supply is enhanced by BESS, DR and DTR systems. In each year of the simulation, the random up/down statuses of OHLs and BESSs, the load demand data modified by DR and the line ratings enhanced by DTR are prepared in advance for the entire year. At each time step, DC-OPF is executed to determine the amount of power flowing into all load busses. If the power capacities are lower than the demand levels, then the energy gap is removed from BESSs; otherwise, the excess power is charged and stored in BESSs. Both discharging and charging cycles are performed with respect to the power ratings and energy capacity of BESSs.

B. DEMAND RESPONSE MODELLING DETAILS

The PS and FV techniques are implemented in the DR model given their capability to conserve the total energy demand whilst flattening the load profiles to improve the security of supply [29] by shaving away energy above a certain percentage of peak load and filling them in durations with low energy demand (i.e. with low percentage of peak load). Those instances where energy is shaved and filled are known as on-peak and off-peak hours, respectively. The mechanism of the DR function implemented in this paper is formulated as

$$\overline{L(t)}=\begin{cases}P & t\in\{\psi_S:(L(t)>x\%\times\max[L(t)])\}\\ L(t)+A & t\in\{\psi_F:(L(t)<y\%\times\max[L(t)])\},\end{cases} \tag{3}$$

such that

$$y<x, \tag{3a}$$

$$P=x\%\times\max[L(t)], \tag{3b}$$

$$A=\frac{\sum_{t\in\psi_S}(L(t)-P)}{N=\sum_{t\in\psi_F}n}, \tag{3c}$$

where in (3), the modified load curve, $\overline{L(t)}$, is limited to P in all on-peak hours, ψ_S. An on-peak hour is recorded when the original load curve, $L(t)$, exceeds $x\%$ of the peak load, $\max[L(t)]$. The amount of load shaved is recovered during off-peak hours, ψ_F, by an amount defined as A when $L(t)$ falls below $y\%$ of $\max[L(t)]$.

In (3a), the inequality constraint guarantees that y is always lower than x to ensure that there is enough space to fill shaved loads, to avoid the creation of new peaks and to obtain load curves that are as flat as possible. Given that such combination is difficult to determine, various combinations of x and y values and their effects on EENS and BESS utilisations are explored in the Results section. In (3b), the value of P is defined to be equal to $x\%$ of the peak load. In (3c), A is defined as the equal division of the total amount of shaved load during on-peak hours, given by $\sum_{t\in\psi_S}(L(t)-P)$, among all N numbers of off-peak hours, where n is each off-peak hour.

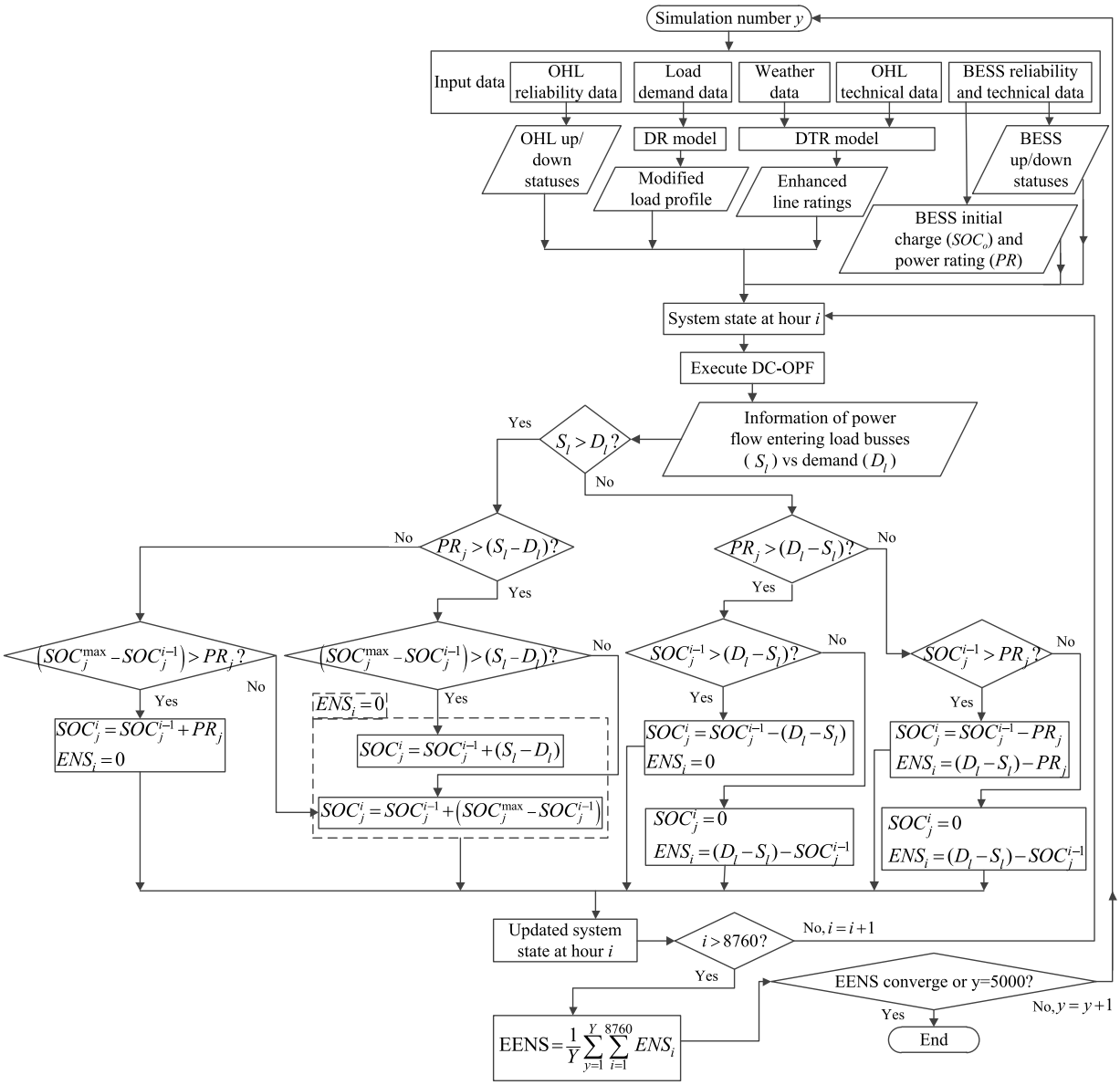

FIGURE 2. Algorithm of the proposed method for evaluating EENS.

C. DTR SYSTEM MODELLING DETAILS

The ratings of transmission corridors enhanced by the DTR system are determined and updated hourly based on the IEEE 738 standard [30] as follows:

$$I = \sqrt{\frac{q_c(\theta, T_a, V_w, \varphi) + q_r(\theta, T_a) - q_s}{R(\theta)}}, \tag{4}$$

where the steady state line current value, I, in ampere is determined based on the balanced convection heat loss, q_c, radiated heat loss, q_r, and solar radiation heat gain, q_s. q_c is calculated based on the designed operating temperature (DOT) of the conductor, θ, ambient temperature, T_a, wind velocity, V_w, and incident wind angle, φ. q_r is affected only by two parameters, namely, θ and T_a. The resistance of the conductor is also considered, and its value changes based on the stipulated DOT, θ. The determined values of I are converted into three-phase power based on the voltage level, V, at which the lines are operating (i.e. $\sqrt{3}\,VI$).

Transmission corridors are usually located far from one another; therefore, the weather characteristics that affect each corridor are unique. In this case, the weather data needed for calculating DTR on each corridor are sampled from 250 km radius locations. Furthermore, given that the length of each transmission corridor is usually several tens of kilometres and that the weather conditions in the same location considerably fluctuate along the distance of the corridor, separate weather

data for every consecutive 10 km radius along each corridor are sampled to recognise these fluctuations. The sampled weather data are then overlaid onto the investigated power network.

Following the sampling criteria, the historical wind speed and angle values for 20 years (from 2000 to 2019) are obtained from the British Atmospheric Data Center (BADC) [31]. However, these historical wind data are limited, and given that the required number of iterations for the convergence of the SMC simulation exceeds the sampled weather data, these data are fitted into the auto-regressive moving-average (ARMA) model due to its ability to simulate an unlimited number of wind values, thereby satisfying the input requirement of the SMC simulation. The ARMA model is also chosen due to its suitability for fitting time series data [32], which match the format of the sampled wind speed and angle values. During the fitting process, the ARMA model considers the historical and random features of the data and then uses such information to randomly simulate their values whilst retaining the original propagation pattern of the data. This simulation feature of the ARMA model is realistic given that the future weather values are most likely different yet their unfolding and propagation patterns are mostly similar. For example, the seasonal changes in weather conditions always follow the winter–spring–summer–autumn sequence, but their values may randomly vary within each season and hence are difficult to predict. The inherent random simulation feature of the ARMA model also contributes to a probabilistic study, which is the key purpose of performing SMC simulations.

This ARMA fitting process is not performed for ambient temperature, T_a, given that temperature is stable throughout each season and covers a very large area. Therefore, only the highest temperature in each season as recorded in the historical data is used to calculate DTR for the sake of simplicity. Solar radiation angle and intensity are also based on conservative values specified in IEEE 738 given that their effects are much weaker than that of wind in the DTR calculations [33].

The ARMA models of wind speed and angle are formulated as [32], [34]:

$$y_t = \alpha_1 y_{t-1} + \alpha_2 y_{t-2} + \cdots + \alpha_m y_{t-m} + e_t - \beta_1 e_{t-1} - \beta_2 e_{t-2} - \cdots - \beta_n e_{t-n}, \quad (5)$$

where α_m and β_n are the m-order auto-regressive and n-order moving-average constants of the ARMA model, respectively, e_t is the normal white noise coefficient that accounts for the probabilistic simulations of wind speed/angle such that this coefficient is normally and independently distributed (NID) and centred at zero with σ^2 variance (i.e. $e_t \in \text{NID}\left(0, \sigma^2\right)$) and y_t is the simulated wind speed or angle values whose timestamps are denoted by subscript t. The above equation shows that the simulations of a particular y_t depends on m past simulated values (i.e. $y_{t-1}, y_{t-2}, \ldots, y_{t-m}$) and n past random coefficients (i.e. $e_{t-1}, e_{t-2}, \ldots, e_{t-n}$).

The correlations of all sampled wind data are considered during the simulations of ARMA models by combining the univariate normal distribution of each individual ARMA model into a multivariate normal distribution as follows:

$$\text{V}(e_t) = \frac{\exp\left\{-\frac{1}{2}(x-\mu)^{\text{T}}\,\Sigma^{-1}\,(x-\mu)\right\}}{(2\pi)^{p/2}\,|\Sigma|^{1/2}}, \quad (6)$$

where p is the number of ARMA models, μ is the zero mean vector that collects the mean values of all ARMA models, Σ is the symmetry covariance matrix whose entries include the correlations amongst all ARMA models and x is a random vector with the same size as μ. Equation (6) yields a vector of the correlated random values of all ARMA models, $\text{V}(e_t)$.

Therefore, by substituting the random e_t generated from (6) into (5), the wind speed and angle values that consider the correlations amongst the historical sampled data are simulated. Afterwards, the simulated weather values are substituted into (4) to yield the DTRs of all lines, which are also correlated in the same manner. Fig. 3 presents sample simulated DTRs for a week (168 hours) and highlights the maximum, mean and minimum values of DTR and STR. In determining DTRs, the physical properties of the Drake Aluminium Conductor Steel Reinforce (ACSR) are used along with one of its DOTs (75 °C). The other possible DOTs of ACSR are either 50 °C or 65 °C [35]. The STR is determined based on the 1% probability of exceeding actual line ratings [36], which are also the simulated DTRs. Fig. 3 shows that STR substantially undermines the capacity potential of lines and causes line overloading in some instances.

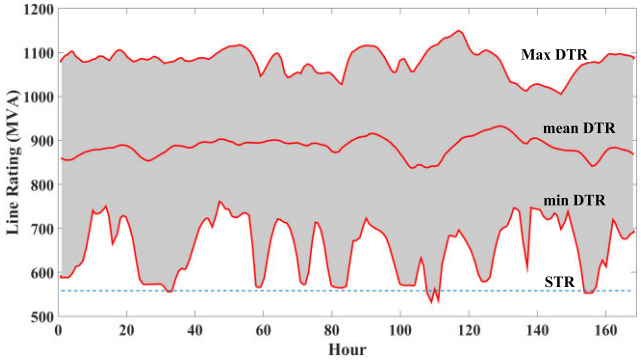

FIGURE 3. Algorithm of the proposed method for evaluating EENS.

D. BESS MODELLING DETAILS

The BESSs modelled in this paper are owned by utilities and deployed on all load buses to support the load demands and enhance the security of supply. Given that the power supply, S_l, entering load bus l and that the demand level, D_l, of the load bus are determined and known at every simulation hour i, the SOC of BESS j, SOC_j^i, is updated based on one of

the following conditions whilst taking the power ratings, PR_j, of BESS into consideration:

1) The supply is greater than the demand, $S_l > D_l$, the BESS is ready for charging, the potential for energy storage, $R_j^{i-1} = SOC_j^{max} - SOC_j^{i-1}$, is known, and
   a) the BESS power rating is less than the supply–demand mismatch, $PR_j < (S_l - D_l)$:

$$\begin{aligned} SOC_j^i &= SOC_j^{i-1} + R_j, \quad R_j^{i-1} < PR_j \\ SOC_j^i &= SOC_j^{i-1} + PR_j, \quad R_j^{i-1} > PR_j, \end{aligned} \tag{7}$$

   b) the BESS power rating is greater than the supply–demand mismatch, $PR_j > (S_l - D_l)$:

$$\begin{aligned} SOC_j^i &= SOC_j^{i-1} + R_j, \quad R_j^{i-1} < (S_l - D_l) \\ SOC_j^i &= SOC_j^{i-1} + (S_l - D_l), \quad R_j^{i-1} > (S_l - D_l), \end{aligned} \tag{8}$$

where (7) shows the surplus of power supply and highlights battery power rating as a limiting factor that determines the maximum charging power at any period even when the remaining battery storage room can sufficiently store all surplus power. In instances when the remaining storage room drops below the power rating, the storage room becomes the limiting factor in determining the charging power level. By contrast, in (8), given that the power rating exceeds the surplus power supply, the amount of energy saved depends entirely on the remaining storage room.

2) The supply is less than the demand, $S_l < D_l$, the BESS is ready for discharging and
   a) the BESS power rating is less than the demand gap, $PR_j < (D_l - S_l)$:

$$\begin{aligned} SOC_j^i &= 0, \quad SOC_j^{i-1} < PR_j \\ SOC_j^i &= SOC_j^{i-1} - PR_j, \quad SOC_j^{i-1} > PR_j, \end{aligned} \tag{9}$$

   b) the BESS power rating is greater than the demand gap, $PR_j > (D_l - S_l)$:

$$\begin{aligned} SOC_j^i &= 0, \quad SOC_j^{i-1} < (D_l - S_l) \\ SOC_j^i &= SOC_j^{i-1} - (D_l - S_l), \quad SOC_j^{i-1} > (D_l - S_l), \end{aligned} \tag{10}$$

where (9) shows a power supply shortage and that the battery power rating is smaller than the power gap. Therefore, the power rating is the limiting factor that determines the amount of power that the battery can discharge to support load demand at any period. The battery storage is depleted when the current energy stored is less than the power rating. By contrast, in (10), the power rating exceeds the power gap. Therefore, the current energy stored in the battery determines the amount of discharging power when supporting load demand.

A level of maintenance SOC is also considered, which is fixed at 20% of the BESS maximum SOC at all times.

III. CASE STUDY

The investigated transmission network is based on the IEEE 24-bus reliability test network (RTN) [37]. All loads and generations are increased by fivefold to stress the network capacity and to highlight the benefits of DR, DTR and BESS. This increment in load level also represents future scenarios of demand increase. The RTN produces a load profile every hour for one year whilst considering seasonal load consumption behaviour.

Given that the RTN is separated into two voltage levels (138 kV and 230 kV), two types of ACSRs are deployed in each voltage level according to their voltage capacity and typical conductor deployment choice. The Drake and Lapwing ACSRs [38] constitute the lower and higher voltage networks, respectively. The weather data required for calculating DTR are obtained from the BADC on an hourly basis from 2000 to 2019 according to the sampling rule mentioned in Section II.C and are overlaid onto the RTN.

Although RTN is a relatively small network that is not representative of any specific power system, the characteristics used in designing the network are universal and hence provide useful references for testing the impacts of various applications, technologies and evaluation techniques; given these designing criteria, the RTN represents as much as possible the different technologies and configurations that can be encountered in any power system [37]. Moreover, the complete reliability data presented in the RTN is difficult to obtain elsewhere, and using other kinds of network would render the reliability evaluation performed in this paper impossible.

IV. RESULTS AND DISCUSSIONS

A. IMPACT OF BESS ENERGY CAPACITY AND POWER RATING

The method and modelling details described in Section II are used to estimate the impact of storage on the EENS of the RTN. The energy capacity considered by BESS ranges from 20 MWh to 100 MWh, and the power rating ranges from 4 MW to 80 MW. Due to the maintenance SOC requirement (20% of the energy capacity), the maximum power rating of each energy capacity level is limited to 80% of the full energy capacity. BESS is considered fully reliable here. DR is implemented on the load demand profile at three percentages of peak load (i.e. 5%, 10% and 20%). All aforementioned BESS and DR settings are implemented on the RTN with and without the DTR system (based on mean values of simulated DTRs), and the results are shown in Figs. 4 and 5, respectively.

Results show that increasing the capability of BESS (i.e. energy capacity and power rating) improves the EENS of the network regardless of whether the DTR is employed or not. This finding can be ascribed to the fact that a BESS with high capacity and power rating can support more load demand and thereby reduce load curtailment. In the above figures, the EENS of the network improves as the percentage of DR increases. A higher DR percentage produces lower

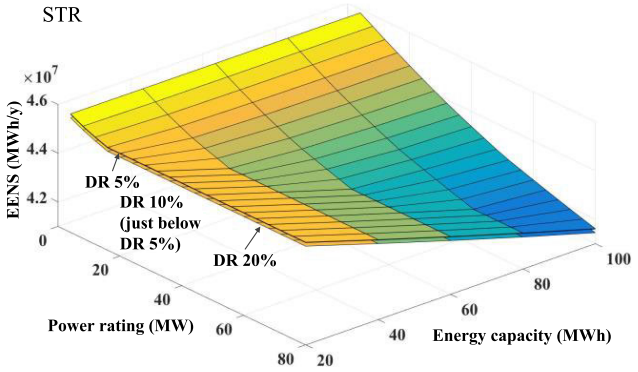

FIGURE 4. Impact of BESS on EENS alongside DR and STR.

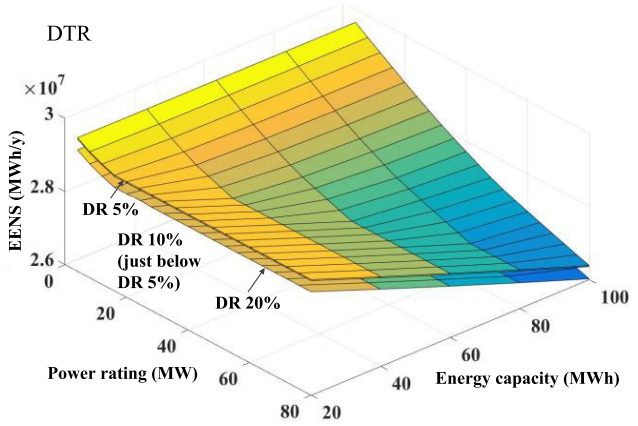

FIGURE 5. Impact of BESS on EENS alongside DR and DTR.

peaks by shifting peak loads to off-peak hours and, as a result, improves the adequacy of power supply and reduces EENS. However, a too high DR percentage can create new peak loads and may eventually be detrimental to the reliability of the power network. Such factor is investigated in Section IV. D.

A comparison of Figs. 4 and 5 clearly shows that the network operating with STR has a much worse EENS than that operating with DTR. Therefore, the additional power capacity of the network unlocked by the DTR system can deliver significantly more power supply to load points, thereby subsequently reducing the EENS. The percentage improvement in the EENS values is evaluated and shown in Fig. 6, which reveals that the greatest improvement is recorded at 37.2% when the capability of BESS reaches its peak and the percentage of DR is at 20%. By contrast, when the capability of BESS and percentage of DR are at their lowest, the improvement in EENS reaches its lowest level at 35.4%. In general, Fig. 6 points out that higher BESS capability and DR percentage levels correspond to a higher percentage improvement in EENS.

These results can be used to establish a boundary for BESS energy capacity and power rating, with the acceptable level of EENS left to the discretion of power system operators.

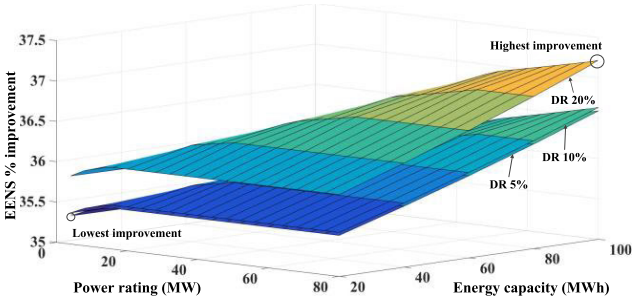

FIGURE 6. Percentage improvement of EENS.

B. IMPACT OF LOAD LEVELS

The results in Figs. 4 and 5 are obtained based on the load level (LL) that has been increased fivefold. Such level of LL increment is reduced in this section to examine the effects of low LLs on EENS. The maximum power rating of each energy capacity level of BESS is used, DR is implemented at 20% of the peak load and the mean simulated DTR are observed. The results are presented in Fig. 7, which shows that lower LLs contribute to lower EENS on average by as much as 10.9% in LL2 and 22.3% in LL3 across all BESS energy capacities.

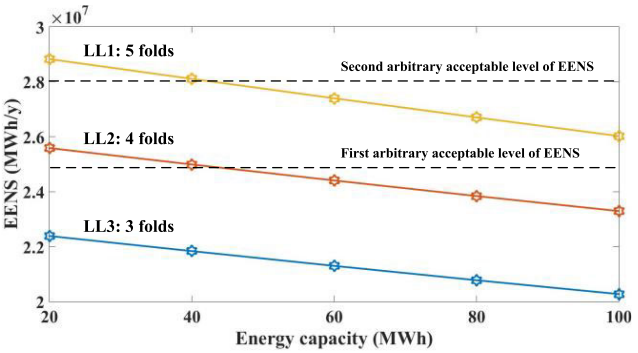

FIGURE 7. Effects of various LLs on EENS, with maximum BESS power ratings at each energy capacity level, DR at 20% peak load, and mean values of DTR.

According to the first arbitrary acceptable level of EENS, which in practice is based on the discretion of system operators, the BESS energy capacity can be minimised under the LL3 scenario and still satisfy the acceptable threshold of EENS. However, the energy capacity of BESS must be at least 50 MWh and above in the LL2 scenario to stay below the acceptable EENS threshold. Meanwhile, in the LL1 scenario and with the first EENS threshold being upheld, none of the BESS capacity levels can steer clear of violating the threshold. The LL1 scenario requires new asset investments, such as new lines, cables or transformer connections. However, if the second arbitrary acceptable level of EENS is used, then both the LL2 and LL3 scenarios are completely safe from violating the threshold regardless of the employed BESS capacity. In the LL1 scenario, a BESS of at least 50 MWh is

required to stay below the second arbitrary acceptable level of EENS threshold.

Fig. 7 presents system operators an estimate of how long their BESS deployments can maintain a safe/acceptable level of reliability relative to the EENS thresholds. In practice, these thresholds may represent a level in which a substantial power outage or financial loss can occur, and crossing these thresholds is either unacceptable or risky such that the probability of causing cascading blackouts is substantially high.

C. IMPACT OF BESS RELIABILITY

The results presented in the previous sections are based on BESSs with 100% reliability. This section explores the reliability impact of BESS on EENS based on the maximum power rating at each energy capacity level of BESS, the DR implemented at 20% of peak load, LL1 and the mean values of simulated DTR. The results are presented in Fig. 8, which shows that the EENS deteriorates (i.e. increases) as the reliability of BESS reduces from 100% to 85%. Interestingly, this effect becomes more apparent as the energy capacity of BESS increases. Initially, increasing the capacity of BESS has a greater impact than increasing its reliability. For example, the percentage increase in EENS at 100 MWh energy capacity from 100% to 85% reliable BESS is about 2% compared to only about 0.37% at 20MWh energy capacity. The BESSs with larger capacity store more charges than those with smaller capacity. When those BESSs with larger capacity become unavailable, the RTN loses more power supply than when those BESSs with lower capacity become unavailable. The loss in power supply subsequently reduces power supply adequacy. Therefore, the negative effects of larger BESSs on EENS are much greater than those of their smaller counterparts.

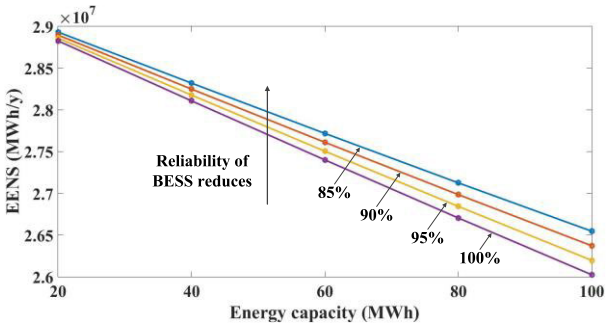

FIGURE 8. Effects of BESS reliability on EENS with the maximum BESS power ratings, DR at 20% peak load, LL1 and mean values of DTR.

Fig. 8 also shows that splitting the large-capacity BESSs into small modules can help prevent sudden power supply loss. Although larger BESSs produce lower EENS than smaller ones, their network reliability benefits fluctuate more than those of smaller BESSs during events of unavailability as shown in Fig. 8. To avoid a huge power adequacy loss, system operators can combine several small BESSs to increase their energy capacity as desired.

D. IMPACT OF THE DR PERCENTAGE OF PEAK LOAD

The peak load at which the DR is implemented has thus far focused only on three percentage values (5%, 10% and 20%). This section further explores the effect of applying DR at other percentages of peak load and determines their effects on EENS. In doing so, fully reliable 100 MWh BESSs rated at 10 power rating levels equally spread from 8 MW to 80 MW are considered along with LL1 and the mean simulated DTR. Fig. 9 presents the results.

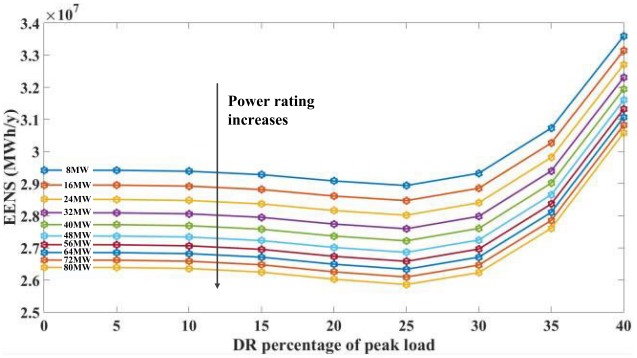

FIGURE 9. Effects of DR percentage of peak load on EENS, with 100MWh BESS at various power ratings, LL1 load level and mean values of DTR.

Fig. 9 shows that in all DR levels, the EENS of the studied network benefits from having BESSs with high power ratings. Interestingly, all BESS ratings show that the reliability of the network improves and that EENS reduces as the percentage of DR increases from 0% to 25%. However, following such increase, these benefits are tapered off and a reversed trend is observed, thereby suggesting that increasing the percentage of the peak load beyond the 25% level during the deployment of DR (i.e. more loads are being shifted) is detrimental to the reliability of the power network. Before reaching the DR 25% level, load shifting generates load profiles that are flatter than the original load profiles, and these profiles help improve the EENS, adequacy and security of the power supply as the number of peak loads and the rating requirements of lines and generators are both reduced. Although a greater amount of peak loads is being shifted after the DR 25% level, the fillings of clipped loads during off-peak hours generate new peaks, which are higher than the original peak loads, as the percentage of DR continuously increases. Therefore, the EENS value increases after reaching the DR 25% level. In short, deploying DR helps improve the load matching ability of BESS, but the improvement stops beyond the 25% peak load level.

Fig. 10 plots a sample load demand profile of the RTN's load bus 8 at DR 0% (no DR deployment), 25% and 40% for 4000 h to illustrate the effects of these DR percentages on peak loads. DR 25% shifts the original peak loads without generating new peaks and creates a flat load profile. However, when DR 40% is deployed, new and huge peak loads are visibly generated; too much loads have been clipped and that there are not enough valleys to accommodate the shifted

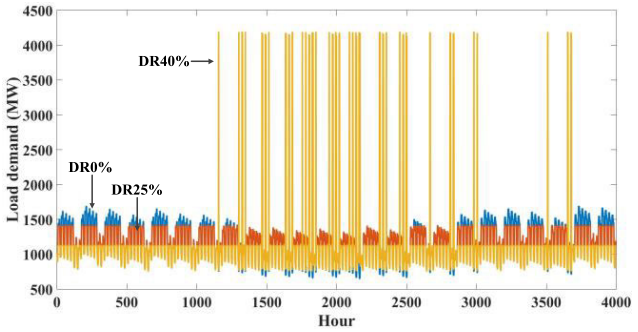

FIGURE 10. Load demand profiles at DR 0%, 25% and 40%.

loads, those peaks that are higher than their original levels are created.

E. IMPACT OF DTR

This section considers the maximum, mean and minimum simulated DTR values along with BESS with a 100 MWh energy capacity. The considered power rating ranges from 4 MW to 80 MW, whereas DR is deployed at a 20% peak load and load level is LL1. Given that the results presented in the previous sections are simulated based on mean DTR values, this section investigates the effects of a wider range of DTR values on the EENS of the investigated power network. Fig. 11 presents the results alongside the STR scenario.

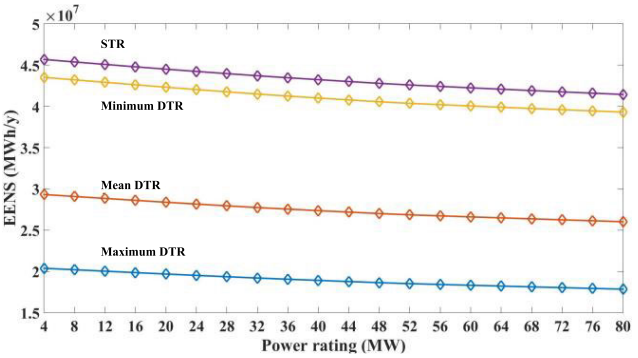

FIGURE 11. Effects of maximum, mean and minimum DTR on EENS with 100 MWh BESS at various power ratings, DR deployed at 20% peak load and LL1.

Fig. 11 shows that when the weather conditions are desirable and when maximum DTR values are produced, the network shows significant improvements in reliability, thereby reducing EENS by 30.9% on average across all power ratings as compared with the mean DTR value scenario. By contrast, compared with the mean DTR value scenario, the minimum DTR value scenario deteriorates the reliability of the network, and the EENS increases by 49.9% on average. Nonetheless, the performance recorded in this scenario is at least 5.2% better than that observed in the STR scenario. Fig. 11 shows that the actual EENS of the network is lower than that recorded in the conventional STR scenario. Even when operating in the mean DTR scenario, which is conservative compared with the maximum DTR scenario, the reliability performance (i.e. EENS) of the network is 36.7% better than that in the STR scenario. Therefore, STR undermines the security of the supply potential of BESS.

F. BESS UTILISATION

Depending on whether the BESS is deployed alongside DR and DTR, the proportion of time that the storage is used and the amount of power discharged to provide security of supply will be affected. These two factors are presented in Figs. 12 and 13, respectively, based on the maximum BESS capabilities (100 MWh and 80 MW), LL1, DR at 25% peak load, STR and the maximum, mean and minimum values of simulated DTR.

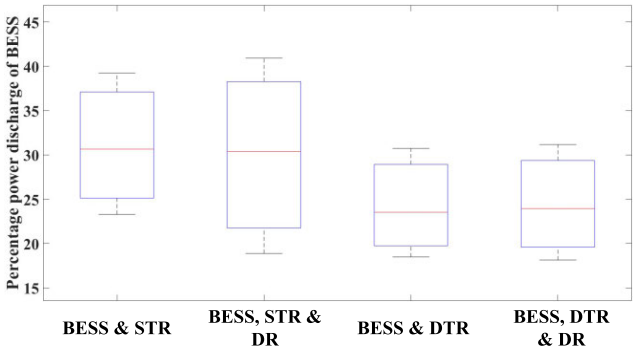

FIGURE 12. Percentage power discharge of BESS alongside DR deployed at 25% of peak load, STR and DTR.

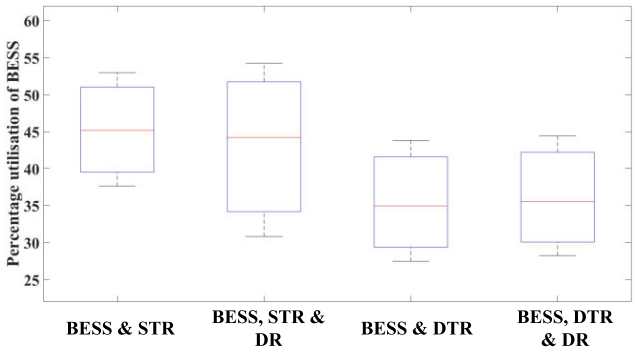

FIGURE 13. Percentage utilisation of BESS alongside DR deployed at 25% of peak load, STR and DTR.

Figs. 12 and 13 show that DTR substantially lowers the percentages of power discharged and utilised by BESS. Fig. 12 shows that the BESSs in the third scenario (operating alongside DTR) discharge 6.8% lesser power on average than those in the first scenario (operating alongside STR). This percentage is calculated by taking the average relative change in the maximum, mean and minimum values between the two scenarios. Meanwhile, Fig. 13 reveals that the BESSs in the third scenario have 9.8% lesser utilisation than those in the first scenario.

The second and fourth scenarios are similar to the first and third scenarios, respectively, except that DR has now been deployed. Figs. 12 and 13 show that DR expands the gap between the maximum and minimum percentages of power discharged and utilised by BESS. The increase in the maximum values can be ascribed to the elevation of valley loads during off-peak hours as a result of the load fillings by peak loads that have been clipped. These valley loads increase the demand for security of supply and subsequently leads to the discharge of additional battery power and an increased utilisation of BESSs. By contrast, the reduction in the minimum values can be ascribed to the clipping of peak loads, which effect is opposite to that of reducing the demand for security of supply, thereby reducing the amount of power discharged from batteries and the utilisation of BESS. These changes are more prevalent than those triggered by the DTR. For example, the maximum values in the second scenario are 1.7% and 1.3% higher than those in the first scenario where STR is deployed as shown in Figs. 12 and 13, respectively, and these differences are only 0.4% and 0.6% lower than those observed in the fourth and third scenarios where DTRs are deployed, respectively. The narrow maximum gaps observed in scenarios with DTR (instead of STR) reveal that the higher power transfer capacity unlocked by DTR can offset the negative effects of load increment during off-peak hours when DR is deployed.

Although the difference between the third and fourth scenarios is not as significant as that between the first and second scenarios, the reliability benefit resulting from the combination of BESS, DTR and DR is substantially better than that observed in the absence of DTR and DR.

V. DISCUSSIONS

The method and results presented thus far support the inclusion of BESSs in transmission networks. This section discusses the implications of these results from the technical, commercial and regulatory perspectives.

A. TECHNICAL IMPLICATIONS

The above results indicate how BESS, DTR and DR and their combinations can improve the security of supply of transmission networks. In the IEEE 24-bus RTN system, the deployments of the DTR system and DR at 25% of peak load can lead to the best security of supply achieved by BESS. The DTR system is also more beneficial in tackling load growth than DR because the demand is most likely to be above STR for most of the time. DTR is also more effective than DR in reducing the utilisation of BESS and the percentage of power discharged for peak matching, thereby allowing BESS to perform additional commercial services and extending its operational lifetime. This extension is vital given that the combination of BESS, DTR and DR can greatly enhance network reliability and withstand high load demands.

However, the future energy requirement of BESS at each period must be known in advance. Consequently, an accurate forecasting of load demand and network ratings, which depend on weather conditions, is crucial. Moreover, BESS needs to perform ancillary services, such as frequency response, and optimising BESS for these services can affect the energy and power requirements of storage. Nonetheless, the proposed method can be used to optimise the energy capacity and power rating of BESS such that there is additional capacity being reserved for ancillary services, with a high certainty that the reserved capacity is not required for security of supply.

B. REGULATORY AND COMMERCIAL IMPLICATIONS

This paper shows that BESS, DTR and DR can reinforce the reliability of transmission networks and that costly asset-based solutions are not necessary. However, the existing network regulations in Saudi Arabia, Malaysia and many parts of the world are not equipped with frameworks that recognise such alternative approach. The proposed method should be considered in these regulations to quantify its benefits and to encourage its adoption. The firm capacity approach employed in most existing methods are not suitable for BESS, DTR or DR. Instead, a probabilistic-risk-based approach is preferred as demonstrated in this paper.

The proposed probabilistic-based method can be used to generate network performance data during a full economic appraisal. This economic analysis enables cost–benefit comparisons with alternative solutions and asset-based strategies. Although the results presented here are directly applicable, a full economic analysis is outside the scope of this paper given that such analysis is affected by many factors other than BESS, DTR and DR. BESS is most likely used to provide ancillary services when not matching peak loads, and many of these services are currently fulfilled by existing generators. To incentivise the adoption of BESSs and to create a market that is conducive to such adoption, the existing regulations and terms should be changed. Consequently, if BESS is favoured over other transmission network reinforcement methods, then the regulations must be changed either to allow network operators to own and operate storage devices or to create a new system that allows third-party BESS operators to engage in contract with network operators and provide peak matching services, thereby improving the security of supply, which can be part of the transmission network ancillary service market.

VI. CONCLUSION

This paper presents a new probabilistic assessment method for determining the appropriate size (energy capacity and power rating) of BESSs in peak matching applications to enhance the security of supply of transmission networks. This method considers the variability of demand and line ratings, the energy and power limitations of storage, the reliability of BESSs and the different DR percentages of peak load deployment.

This paper is the first to examine and quantify the combined benefits of BESS, DTR and DR to the security of supply of transmission networks. The benefits of a combination of

these technologies are greater than their individual benefits, and both DTR and DR can relieve the utilisation of BESS in peak matching applications, thereby subsequently extending its lifetime and allowing its use in other commercial and ancillary services.

The security of supply of the system improves along with the energy capacity and power rating of BESS. The reliability of BESS also becomes a significant factor when its size reaches a level where its capability to match the peak load becomes significant. DTR and DR increase the value of BESS and reduce the requirements of BESS energy capacity and power rating without adversely affecting network reliability. The technical, regulatory and commercial barriers that inhibit the widespread adoption of BESS are also discussed along with some potential solutions.

Finally, it is worth noting that the impacts of charging/discharging frequency and the amount of power exchanged during each cycle towards the operable lifetime of the BESS are never considered in this paper, which should be taken into account as future studies.

REFERENCES

[1] F. Mohamad and J. Teh, "Impacts of energy storage system on power system reliability: A systematic review," *Energies*, vol. 11, no. 7, p. 1749, Jul. 2018.
[2] F. Mohamad, J. Teh, C.-M. Lai, and L.-R. Chen, "Development of energy storage systems for power network reliability: A review," *Energies*, vol. 11, no. 9, p. 2278, Aug. 2018.
[3] J. Teh and C.-M. Lai, "Reliability impacts of the dynamic thermal rating and battery energy storage systems on wind-integrated power networks," *Sustain. Energy, Grids Netw.*, vol. 20, Dec. 2019, Art. no. 100268.
[4] J. Teh, "Adequacy assessment of wind integrated generating systems incorporating demand response and battery energy storage system," *Energies*, vol. 11, no. 10, p. 2649, Oct. 2018.
[5] F. Mohamad, J. Teh, and H. Abunima, "Multi-objective optimization of solar/wind penetration in power generation systems," *IEEE Access*, vol. 7, pp. 169094–169106, 2019.
[6] N. S. Wade, P. C. Taylor, P. D. Lang, and P. R. Jones, "Evaluating the benefits of an electrical energy storage system in a future smart grid," *Energy Policy*, vol. 38, no. 11, pp. 7180–7188, Nov. 2010.
[7] A. Oudalov, R. Cherkaoui, and A. Beguin, "Sizing and optimal operation of battery energy storage system for peak shaving application," in *Proc. IEEE Lausanne Power Tech*, Jul. 2007, pp. 621–625.
[8] M. Nick, M. Hohmann, R. Cherkaoui, and M. Paolone, "Optimal location and sizing of distributed storage systems in active distribution networks," in *Proc. IEEE Grenoble Conf.*, Jun. 2013, pp. 1–6.
[9] S. A. Arefifar and Y. A.-R.-I. Mohamed, "DG mix, reactive sources and energy storage units for optimizing microgrid reliability and supply security," *IEEE Trans. Smart Grid*, vol. 5, no. 4, pp. 1835–1844, Jul. 2014.
[10] P. F. Lyons, N. S. Wade, T. Jiang, P. C. Taylor, F. Hashiesh, M. Michel, and D. Miller, "Design and analysis of electrical energy storage demonstration projects on UK distribution networks," *Appl. Energy*, vol. 137, pp. 677–691, Jan. 2015.
[11] Z. Y. Gao, P. Wang, L. Bertling, and J. H. Wang, "Sizing of energy storage for power systems with wind farms based on reliability cost and wroth analysis," in *Proc. IEEE Power Energy Soc. Gen. Meeting*, Jul. 2011, pp. 1–7.
[12] J. Xiao, L. Bai, F. Li, H. Liang, and C. Wang, "Sizing of energy storage and diesel generators in an isolated microgrid using discrete Fourier transform (DFT)," *IEEE Trans. Sustain. Energy*, vol. 5, no. 3, pp. 907–916, Jul. 2014.
[13] Y. V. Makarov, P. Du, M. C. W. Kintner-Meyer, C. Jin, and H. F. Illian, "Sizing energy storage to accommodate high penetration of variable energy resources," *IEEE Trans. Sustain. Energy*, vol. 3, no. 1, pp. 34–40, Jan. 2012.
[14] Q. Li, R. Ayyanar, and V. Vittal, "Convex optimization for Des.planning and operation in radial distribution systems with high penetration of photovoltaic resources," *IEEE Trans. Sustain. Energy*, vol. 7, no. 3, pp. 985–995, Jul. 2016.
[15] S. You, C. Traeholt, and B. Poulsen, "Economic dispatch of electric energy storage with multi-service provision," in *Proc. Conf. IPEC*, Oct. 2010, pp. 525–531.
[16] E. Rodas-Gallego and D. Mejia-Giraldo, "Market-based impact of a demand response program in the colombian power market," *IEEE Latin Amer. Trans.*, vol. 18, no. 03, pp. 537–544, Mar. 2020.
[17] H. Jabir, J. Teh, D. Ishak, and H. Abunima, "Impacts of demand-side management on electrical power systems: A review," *Energies*, vol. 11, no. 5, p. 1050, Apr. 2018.
[18] H. J. Jabir, J. Teh, D. Ishak, and H. Abunima, "Impact of demand-side management on the reliability of generation systems," *Energies*, vol. 11, no. 8, p. 2155, Aug. 2018.
[19] *IEEE Standard for Calculating the Current-Temperature of Bare Overhead Conductors*, IEEE Standard 738-2006 (Revision of IEEE Std 738-1993), 2007, p. c1-59.
[20] J. Teh, C.-M. Lai, N. A. Muhamad, C. A. Ooi, Y.-H. Cheng, M. A. A. Mohd Zainuri, and M. K. Ishak, "Prospects of using the dynamic thermal rating system for reliable electrical networks: A review," *IEEE Access*, vol. 6, pp. 26765–26778, 2018.
[21] J. Teh, C.-M. Lai, and Y.-H. Cheng, "Impact of the real-time thermal loading on the bulk electric system reliability," *IEEE Trans. Rel.*, vol. 66, no. 4, pp. 1110–1119, Dec. 2017.
[22] J. Teh, "Uncertainty analysis of transmission line end-of-life failure model for bulk electric system reliability studies," *IEEE Trans. Rel.*, vol. 67, no. 3, pp. 1261–1268, Sep. 2018.
[23] J. Teh and I. Cotton, "Reliability impact of dynamic thermal rating system in wind power integrated network," *IEEE Trans. Rel.*, vol. 65, no. 2, pp. 1081–1089, Jun. 2016.
[24] J. Teh and C.-M. Lai, "Risk-based management of transmission lines enhanced with the dynamic thermal rating system," *IEEE Access*, vol. 7, pp. 76562–76572, 2019.
[25] J. Teh and C.-M. Lai, "Reliability impacts of the dynamic thermal rating system on smart grids considering wireless communications," *IEEE Access*, vol. 7, pp. 41625–41635, 2019.
[26] J. Teh, C.-M. Lai, and Y.-H. Cheng, "Improving the penetration of wind power with dynamic thermal rating system, static VAR compensator and multi-objective genetic algorithm," *Energies*, vol. 11, no. 4, p. 815, Apr. 2018.
[27] J. Teh, C. Ooi, Y.-H. Cheng, M. Atiqi Mohd Zainuri, and C.-M. Lai, "Composite reliability evaluation of load demand side management and dynamic thermal rating systems," *Energies*, vol. 11, no. 2, p. 466, Feb. 2018.
[28] N. M. Pindoriya, P. Jirutitijaroen, D. Srinivasan, and C. Singh, "Composite reliability evaluation using Monte Carlo simulation and least squares support vector classifier," *IEEE Trans. Power Syst.*, vol. 26, no. 4, pp. 2483–2490, Nov. 2011.
[29] M. Fotuhi-Firuzabad and R. Billinton, "Impact of load management on composite system reliability evaluation short-term operating benefits," *IEEE Trans. Power Syst.*, vol. 15, no. 2, pp. 858–864, May 2000.
[30] *IEEE Standard for Calculating the Current-Temperature Relationship of Bare Overhead Conductors*, IEEE Standard 738-2012 (Revision of IEEE Std 738-2006 - Incorporates IEEE Std 738-2012 Cor 1-2013), 2013, pp. 1–72.
[31] *British Atmospheric Data Center (BADC)*. Accessed: May 10, 2020. [Online]. Available: http://badc.nerc.ac.uk/data/ukmo-midas/WPS.html
[32] A. M. L. da Silva, L. A. F. Manso, S. A. Flávio, M. A. da Rosa, and L. C. Resende, "Composite reliability assessment of power systems with large penetration of renewable sources," in *Reliability and Risk Evaluation of Wind Integrated Power Systems*, R. Billinton, R. Karki, and A. Verma, Eds. New Delhi, India: Springer, 2013.
[33] M. Siler, J. Heckenbergerova, P. Musilek, and J. Redway, "Sensitivity analysis of conductor current-temperature calculations," in *Proc. 26th IEEE Can. Conf. Electr. Comput. Eng. (CCECE)*, May 2013, pp. 1–4.
[34] R. Karki, P. Hu, and R. Billinton, "A simplified wind power generation model for reliability evaluation," *IEEE Trans. Energy Convers.*, vol. 21, no. 2, pp. 533–540, Jun. 2006.
[35] K. Kopsidas, A. Kapetanaki, and V. Levi, "Optimal demand response scheduling with real-time thermal ratings of overhead lines for improved network reliability," *IEEE Trans. Smart Grid*, vol. 8, no. 6, pp. 2813–2825, Nov. 2017.

[36] C. F. Price and R. R. Gibbon, "Statistical approach to thermal rating of overhead lines for power transmission and distribution," *IEE Proc. C-Gener., Transmiss. Distrib.*, vol. 130, no. 5, pp. 245–256, Sep. 1983.
[37] C. Grigg, P. Wong, P. Albrecht, R. Allan, M. Bhavaraju, R. Billinton, Q. Chen, C. Fong, S. Haddad, S. Kuruganty, W. Li, R. Mukerji, D. Patton, N. Rau, D. Reppen, A. Schneider, M. Shahidehpour, and C. Singh, "The IEEE reliability test system-1996. A report prepared by the reliability test system task force of the application of probability methods subcommittee," *IEEE Trans. Power Syst.*, vol. 14, no. 3, pp. 1010–1020, Aug. 1999.
[38] R. Thrash, A. Nurrah, M. Lancaster, and K. Knuckles, *Overhead Conductor Manual*. Carrollton, GA, USA: Southwire, 2007.

MOHAMED KAMEL METWALY received the B.Sc. (Hons.) and M.Sc. degrees in electrical engineering from Menoufia University, Shebin El-Kom, Egypt, in 1999 and 2003, respectively, and the Ph.D. degree (Hons.) in electrical engineering from the Vienna University of Technology, Vienna, Austria, in 2009. In 2000, he was an Instructor with the Department of Electrical Engineering, Faculty of Engineering, Menoufia University, and an Assistant Lecturer in 2003. From 2010 to 2015, he was a Lecturer with the Department of Electrical Engineering, Faculty of Engineering, Menoufia University, where he was an Assistant Professor from 2015 to 2020 and a Professor in control of electric machines in 2020. His research interests include control of ac machines, applications of power electronics, power factor correction converters, sensorless control of electric drives, renewable energy applications, stability analysis of control systems, observers and estimators, and digital signals processing-based real-time control.

JIASHEN TEH (Member, IEEE) received the B.Eng. (Hons.) in electrical and electronic engineering from Universiti Tenaga Nasional (UNITEN), Malaysia, in 2010, and the Ph.D. degree in electrical and electronic engineering from The University of Manchester, Manchester, U.K., in 2016.

Since 2016, he has been a Senior Lecturer/Assistant Professor with the Universiti Sains Malaysia (USM), Malaysia. In 2018, he was an Adjunct Professor with the Green Energy Electronic Center, National Taipei University of Technology (Taipei Tech), Taipei, Taiwan. Since 2019, he has been an Adjunct Professor with the Intelligent Electric Vehicle and Green Energy Center, National Chung Hsing University (NCHU), Taichung, Taiwan. His research interests include probabilistic modeling of power systems, grid-integration of renewable energy sources, and reliability modeling of smart grid networks.

Dr. Teh is a member of the IEEE Power and Energy Society, the Institution of Engineers Malaysia (IEM), and the Institution of Engineering and Technology (IET). He is also a Chartered Engineer (C.Eng.) with the Engineering Council, U.K., and a registered Professional Engineer (P.Eng.) with the Board of Engineers Malaysia (BEM). He received the outstanding publication awards from USM in 2017 and 2018. He serves as a Regular Invited Reviewers for the *International Journal of Electrical Power and Energy Systems*, IEEE Access, the IEEE Transactions on Industry Applications, the IEEE Transactions on Vehicular Technology, the IEEE Transactions on Reliability, the IEEE Transactions on Industrial Electronics, and *IET Generation, Transmission and Distribution*.